

# The optimization topography of exciton transport

TORSTEN SCHOLAK<sup>1,2</sup>, THOMAS WELLENS<sup>1</sup>, AND ANDREAS BUCHLEITNER<sup>1</sup>

<sup>1</sup> *Physikalisches Institut, Albert-Ludwigs-Universität Freiburg, Hermann-Herder-Straße 3, D-79104 Freiburg, Germany, EU*

<sup>2</sup> *Chemical Physics Theory Group, Department of Chemistry and Center for Quantum Information and Quantum Control, University of Toronto, Toronto M5S 3H6, Canada*

PACS 05.60.-k – Transport processes: Transport processes

PACS 87.15.hj – Biomolecules: structure and physical properties: Transport dynamics

PACS 03.65.Yz – Quantum mechanics: Decoherence; open systems; quantum statistical method

**Abstract.** – Stunningly large exciton transfer rates in the light harvesting complex of photosynthesis, together with recent experimental 2D spectroscopic data, have spurred a vivid debate on the possible *quantum* origin of such efficiency. Here we show that configurations of a random molecular network that optimize constructive quantum interference from input to output site yield systematically shorter transfer times than classical transport induced by ambient dephasing noise.

**Introduction.** – A growing amount of experimental data [1–3] suggest that quantum coherence may be at the origin of the stunning efficiency of exciton transport in photosynthetic light harvesting, even at ambient temperatures and in a doubtlessly very noisy environment. The simplest natural structure that exhibits these surprising properties is the Fenna-Matthews-Olson (FMO) light harvesting complex of green sulfur bacteria, which consists of seven (or eight [4]) bacteriochlorophyll molecules arranged in a disordered network [5,6]. Exciton transfer is here mediated by dipole-dipole coupling between these different molecular sites, and is associated with a de-excitation of the donor site from some excited to the ground state, and an excitation of the acceptor site from the ground to some excited state. The molecular network that mediates the exciton transfer, from the antenna complex to the reaction center, where the excitation fuels the organism’s chemistry, is embedded into a complicated protein structure, which seems to provide some structural stiffness, and also defines a nontrivial spectral structure of the environment, which preserves the coherence on the FMO network itself, on considerably longer time scales than to be expected for a white noise environment [7]. Since the prevalence of the coherence effects in widely open systems in contact with high temperature environments challenges our traditional understanding of what seemed the restricted realm of quantum mechanics, these highly specialized biological functional units let us think anew how to control efficient transport in disordered and noisy systems, possibly by ex-

ploiting fundamental quantum features.

The available experimental evidence, still not always fully consistent [1,2] and vividly debated, is mirrored by a large variety of theoretical approaches, which distinguish themselves in terms of the applied methodology as well as of the level of faithfulness of the modeling of the actual biomolecular object under scrutiny—from advanced quantum molecular dynamics [4], over quantum simulations [8–10] based on some effective, seven site Hamiltonian [11], Lindblad equations [12] or various non-Markovian approaches derived from open system theory [13–17], to diverse quantum optical models [18–20] and abstract statistical treatments [21,22]. In essence, there are four principal lines of argument to explain efficient exciton transport, by (i) noise-assisted, (ii) non-Markovian or (iii) driving, and (iv) multi-path interference induced exciton transfer. Given the available experimental data and the hitherto limited characterization and control of the precise microscopic Hamiltonian and environment coupling agents that generate the experimentally observed phenomena, it remains an open question which of these suggested mechanisms were actually used by evolution to optimize the FMO’s functionality. Since any improvement that provides an evolutionary advantage will be implemented, it is even not unlikely that all of them are used at some level. However, in the light of the debate about a possible *quantum* enhancement of transport in the photosynthetic complex, it is highly relevant to understand the specific role of quantum coherence for these different mecha-

nisms, and to compare the achievable transfer efficiencies they allow for. It is the present contribution’s purpose to provide such comparison for noise-enhanced and multi-path-interference transport scenarios. Large scale statistical sampling will allow us to show that multi-path quantum interference always leads to better results than noise-assisted, essentially classical transport processes, though requires additional optimization of the molecular structure. Indeed, this even holds in the presence of not too strong ambient noise, and thus identifies yet another scenario where genuine quantum effects may define an evolutionary advantage.

**Random molecular networks.** – The noise-enhanced as well as the multi-path-interference scenario start out from the same structural elements that are unambiguously given by experimental observations: Exciton transfer occurs across a random molecular network with local sites effectively modeled as electronic two-level systems, and further background degrees of freedom, which may possibly exert some effective driving [18], can in principle be accounted for by some non-Markovian environment coupling [13]. Experimentally observed exciton cross-terms [1], though with quite some experimental scatter [2], suggest excitonic coherence times which exceed the exciton transfer time between antenna and reaction center by a factor two to five [1], even at ambient temperatures [2]. The presently best available effective Hamiltonian, which is inferred from experimental data and advanced quantum chemical model calculations predicts a strong suppression of strictly coherent transport across the FMO complex (approx. 5 % transfer efficiency [21,22]), from the input to the output site, due to predominantly destructive multi-path interference upon transmission.

However, exciton transfer in the FMO complex occurs with efficiencies larger than 95 % [7], and there are essentially two alternative scenarios which can explain this discrepancy between the experimental data and the best microscopic Hamiltonian presently available. Since quantum coherence can be destroyed by ambient noise, and since suppressed transport under purely coherent dynamics can only be due to destructive interference effects, it is very natural to argue in favor of noise-induced transport [23]. Since, however, destructive multi-path interference is known to be very sensitive with respect to changes of the boundary conditions and/or the Hamiltonian’s coupling matrix elements [24], and since even the best available model Hamiltonian for the FMO complex is garnished with appreciable uncertainties for its individual entries [11], one may equally well argue in favor of *constructive* multi-path interference as the observed efficiency’s cause. This even more so since all experimental data that so far lend support for the coherent transport hypothesis are obtained from bulk measurements rather than from single molecule spectroscopy, and therefore might mask much longer coherence times by inhomogeneous broadening effects [3].

Since both alternative explanations allow to predict large transfer efficiencies, let us have a closer look at the respective key mechanisms. We model the energy conserving, unitary dynamics of a single excitation injected into a molecular network alike the FMO complex by the Hamiltonian

$$H = \sum_{i \neq j=1}^7 v_{i,j} |i\rangle \langle j|, \quad (1)$$

with  $|i\rangle$  and  $|j\rangle$  the electronic states where the excitation is localized at the individual molecular sites  $i$  and  $j$ , respectively. We assume that initially only one site, “in”, is excited, which is identified with the first site of the network. The sites No. 2 to 6 are referred to as the “intermediates”. The seventh and last site is the designated output site, “out”, where we add an energy sink, such as to mimic the irreversible exciton absorption at the reaction center. We couple each of the seven molecular sites to a private (*i.e.*, there is no inter-site communication through the environment) dephasing environment. Sink and dephasing induce some irreversibility on the FMO degrees of freedom, which we incorporate by the Lindblad terms

$$L_{\text{sink}}(\varrho) = \Gamma(|0\rangle \langle \text{out}| \varrho | \text{out}\rangle \langle 0| - \frac{1}{2} \{ |\text{out}\rangle \langle \text{out}|, \varrho \}), \quad (2)$$

where  $|0\rangle$  and  $\{, \}$  are the ground state of the molecular network and an anticommutator, respectively, and

$$L_{\text{deph}}(\varrho) = -4\gamma \sum_{i \neq j=1}^7 |i\rangle \langle i| \varrho |j\rangle \langle j| \quad (3)$$

into the effective evolution equation of the excitonic state on the network,

$$\dot{\varrho}(t) = -i[H, \varrho(t)] + L_{\text{sink}}(\varrho(t)) + L_{\text{deph}}(\varrho(t)) \quad (4)$$

(where we have set  $\hbar = 1$  for convenience). To obtain a robust comparison of the different transport mechanisms, we statistically sample the transport efficiency over different realizations of  $H$ , by random sampling over the positions of all intermediate sites, within a sphere with input and output site placed on its north and south pole, respectively. Random positions  $\vec{r}_j$  translate into random realizations of  $H$  by defining the coupling matrix elements as a function of the intersite distances,

$$v_{i,j} = \alpha r_{i,j}^{-3} \quad (5)$$

with some constant  $\alpha$ , and  $r_{i,j} = |\vec{r}_i - \vec{r}_j|$ . By choosing random positions for the intermediate sites, we in some way take into account the experimental uncertainty concerning the actual FMO Hamiltonian [11]. Let us stress, however, that we do not present our model as a realistic description of a particular experiment. On the contrary, we are rather interested in general properties of transport, as they will appear if we allow for a large variety of possible configurations, without imposing, from the very beginning, strict experimental boundary conditions.

The model discussed above has three intrinsic time scales which will largely determine the expected transfer efficiencies—the direct exciton transfer time

$$T = \frac{\pi}{2|v_{\text{in,out}}|} \quad (6)$$

between input and output site, in the absence of all intermediate sites, the local dephasing rate  $4\gamma$  (identical for all sites), and the sink dissipation rate  $\Gamma$ , which we will fix at the value  $\Gamma = 10/T$  in the following <sup>1</sup>. Randomly placed intermediate sites between input and output help to enhance or suppress coherent transport [21, 22], by larger coupling strengths between closer sites and appropriate phase relationships. The dephasing rate defines the time scale  $\mathfrak{T}_{\text{deph}} = (4\gamma)^{-1}$  on which such phase relationships can have a bearing on the overall transport behavior, and the sink dissipation rate defines an optimal time scale on which population has to be delivered to the output site, to make it immediately available for the reaction center.

**Statistics of transport efficiency.** – To compare the transport efficiency provided by different molecular conformations and different dephasing rates, we define the average transfer time

$$\mathfrak{T} = \Gamma \int_0^\infty t p_{\text{out}}(t) dt, \quad (7)$$

which is the expectation value of the time required to transfer the excitation to the sink, determined by the population  $p_{\text{out}}(t) = \langle 0|\dot{\rho}(t)|0\rangle/\Gamma$  of the output site. We see here that the ground state  $|0\rangle$  can only be populated by delivering the exciton from the output site to the sink, with rate  $\Gamma$ , cf. also eq. (2). The shorter the transfer time, the more efficient the transport <sup>2</sup>.

We are now prepared for a statistical analysis of exciton transfer times across a molecular network alike the FMO complex, to assess the potential role of coherent vs. noise-assisted transport mechanisms to steer transport efficiencies. In order to draw a landscape of the exciton transport efficiency in molecular networks as modeled by eq. (4), we sample over fifty million random and distinct conformations. For each conformation in the ensemble the computational procedure involves the following tasks: First, the positions of the five intermediate molecular sites are randomized, which are then used to populate the matrix entries of the Hamiltonian  $H$  according to eq. (5). For values of  $\gamma$  from  $10^{-5}\Gamma$  to  $10^3\Gamma$  in 200 logarithmic steps, *i.e.* for essentially vanishing to very strong dephasing rates, the master equation, eq. (4), is solved via exact

<sup>1</sup>This implies one incoherent event on the time scale  $T/10$ , hence a rather efficient drain. We have used this time scale as an efficiency benchmark in earlier work [21, 22].

<sup>2</sup>Note that  $\mathfrak{T}$  is a reasonable efficiency quantifier if efficiency is qualified as rapid and irreversible excitation transfer to the sink, but that it does not distinguish quantum from classical transport efficiencies, since it integrates over all times. It is however evident that the definition of any efficiency quantifier is a matter of pragmatic choice rather than of principle, and that all such quantifiers call for a careful interpretation

numerical diagonalization and the transfer times  $\mathfrak{T}$  are calculated. The last step employs logarithmic data binning to record the transfer time histogram  $f_{\mathfrak{T}}$ , shown in Fig. 1, as a function of  $\gamma$ . In the left density plot of the figure, the grey scale represents the probability density of configurations giving rise to a certain transfer time, under a given dephasing rate. Configurations above the left hand, decreasing dotted line correspond to transfer times *longer* than  $\mathfrak{T}_{\text{deph}}$ , *i.e.* the exciton transfer is here due to *classical transport* across the network. For even larger dephasing rates, transport is “frozen” due to a Zeno-like projection mechanism ( $\mathfrak{T}_{\text{Zeno}} \propto \gamma$ , as indicated by the increasing dotted line), while configurations below the left hand dotted line achieve efficient transfer on time scales *shorter* than  $\mathfrak{T}_{\text{deph}}$ . The latter thus mediate *coherent exciton transfer* and are the only ones which are eligible for claiming an unambiguous *quantum enhancement* of exciton transfer in the FMO complex. Indeed, the shortest transfer times are observed for a finite subset of these configurations, on the lower left hand side of Fig. 1. If we furthermore optimize the molecular configuration in the absence of any dephasing, for the same sink dissipation, and then expose this optimal configuration to finite dephasing rates, we obtain the dashed curve in Fig. 1, which exhibits exciton transfer times *shorter* than the classical value, associated with the highest density of configurations in the plot, by at least a factor two, for almost all dephasing rates that allow for coherent transfer. Note that this optimal configuration still yields very efficient excitation transfer even for higher dephasing rates, which suggests that the optimized coherent transport on short time scales imparts an initial advantage, even when classical activation takes over on long time scales.

**Discussion.** – The optimization landscape thus provides a clear picture of the possible strategies to achieve efficient transfer across an FMO like, disordered network: The large majority of randomly sampled configurations requires the *assistance of noise* to allow for efficient transport, which, however, will be *classical* in nature, and will occur on time scales clearly longer than  $\mathfrak{T}_{\text{deph}}$ . Indeed, the clustering of all the configurations associated with this transport mechanism around  $\mathfrak{T} \simeq 10/\Gamma = T$  and  $\gamma \simeq \Gamma$  in Fig. 1 expresses an approximate matching condition of dephasing and sink dissipation rates, which is an intrinsically classical, statistical synchronization phenomenon. Excitation transfer here stems from the noise induced destruction of quantum coherence, is induced on time scales *longer* than the system inherent coherence times, and is essentially *independent* of the microscopic Hamiltonian which generates the coherent dynamics on the network (hence the large density of configurations at these transfer times and dephasing rates). Under an evolutionary perspective, this non-selectivity with respect to the microscopic coupling structure can therefore neither define an evolutionary advantage by optimizing the molecular structure—most structures will do, as also highlighted by

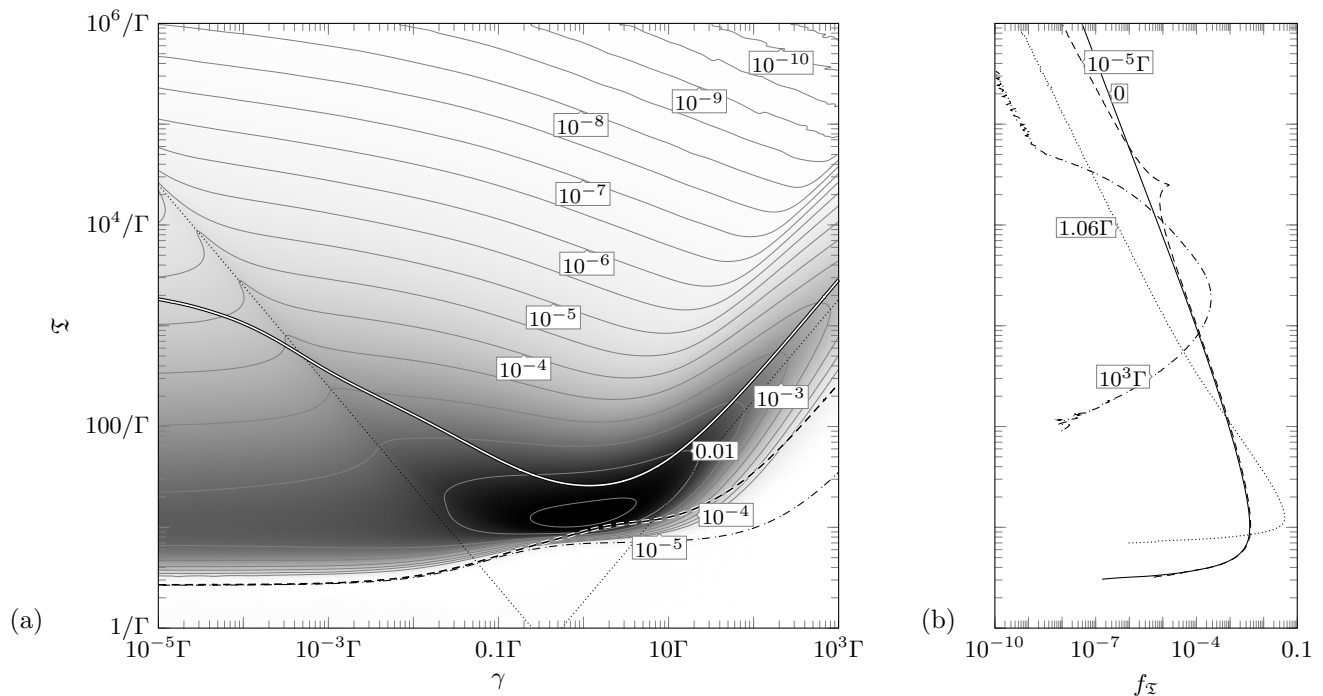


Fig. 1: (a) Probability density  $f_{\tilde{\mathfrak{T}}}$  of the average excitation transfer time  $\tilde{\mathfrak{T}}$ , eq. (7), for  $N = 7$  molecular sites and sink rate  $\Gamma = 10/T$ , as a function of the dephasing rate  $\gamma$ . The two dotted, diagonal lines are given by the dephasing time  $\tilde{\mathfrak{T}}_{\text{deph}} = (4\gamma)^{-1}$ , and by an approximate Zeno time  $\tilde{\mathfrak{T}}_{\text{Zeno}} \propto \gamma$ , respectively. On time scales  $\tilde{\mathfrak{T}} > \tilde{\mathfrak{T}}_{\text{deph}}$ , the purity of the excitonic state on the molecular network has dropped to its minimum value, hence the transport is essentially classical. The white line shows the median  $\tilde{\mathfrak{T}}$ , the dot-dashed line the minimum transfer time, and the dashed line the transfer time of a configuration that has been optimized for  $\gamma = 0$ . (b) Height profiles of the probability densities for fixed dephasing rates  $\gamma = 0$  (solid line),  $10^{-5}\Gamma$  (dashed line),  $1.06\Gamma$  (dotted line),  $10^3\Gamma$  (dash-dotted line).

the pronounced minimum of the median of the distribution (white curve) at  $\gamma \simeq \Gamma$ .

In contrast, Fig. 1 also shows that a small but finite sub-ensemble of *optimal configurations* mediates *efficient quantum transport* of the excitation from input to output, faster than the noise-assisted, classical transport, and due to constructive quantum interference upon transmission, which prevails in the presence of noise, actually in the entire range of dephasing rates considered in Fig. 1. If quantum mechanics is at the origin of the experimentally observed exciton transfer efficiencies in the FMO complex, it therefore must stem from such type of optimal molecular configurations, or otherwise ought to be induced by non-Markovian [14] or driving effects [18]. Since the optimal transfer rates mediated by such optimal configurations define rare events in the statistical sample represented in Fig. 1, it is conceivable that they define an evolutionary advantage which was hardwired by nature. The cusp-like structure that emerges right along the line defined by the dephasing time  $\mathfrak{T}_{\text{deph}}$  highlights molecular configurations which exhibit an eigenstate of  $H$  localized on the site “in” and on another site  $j \neq$  “out”. For these configurations, coherent transmission is suppressed by destructive interference, and hence noise is required to assist the exciton’s delivery at the sink, with transfer times  $\mathfrak{T} = \mathfrak{T}_{\text{deph}}$ .

Let us conclude with a short discussion of the actual structure of optimal configurations in the coherent regime: When investigating the molecular conformations which exhibit transfer times shorter than the dephasing time  $\mathfrak{T}_{\text{deph}}$  in Fig. 1, these show a wide variability as regards their dimensionality and symmetry properties. Minimal transfer times are achieved by near to one dimensional structures, while fully three dimensional and prima facie disordered structures, that mediate optimal coherent transport on closed molecular networks with vanishing sink dissipation, achieve slightly longer transfer times  $\mathfrak{T}$ , though still significantly shorter than the dephasing time. Since Fig. 1 is obtained for a relatively large sink dissipation rate, which corresponds to a significant change of boundary conditions as compared to the closed network, this is not surprising, though raises the question for the actual optimality conditions favored by nature: Besides rapid transfer, also robustness and multifunctionality issues define further constraints which go far beyond the scope of our present model considerations, but define a beautiful and fascinating area for further research. Therefore, it remains an open question, whether nature indeed employs quantum coherence to benefit energy transport in photosynthesis by having evolved molecular conformations corresponding to the optimal configurations discovered here. It appears that due to the strong sensitivity of the transport efficiency on the particular realization of disorder this question can only be answered by a highly precise measurement of the electronic Hamiltonian with an accuracy beyond what is accessible today. Finally, regardless of whether the near-to-perfect efficiency of the FMO complex is truly caused by quantum coherence or not, the existence of optimal con-

figurations achieving maximum performance due to constructive quantum interference will certainly spur the design of new experiments and, in the long run, advanced devices such as a new generation of organic solar cells that utilize the beneficial aspects of quantum coherence.

## REFERENCES

- [1] ENGEL G. S., CALHOUN T. R., READ E. L., AHN T.-K., MANCAL T., CHENG Y.-C., BLANKENSHIP R. E. and FLEMING G. R., *Nature*, **446** (2007) 782.
- [2] PANITCHAYANGKON G., HAYES D., FRANSTED K. A., CARAM J. R., HAREL E., WEN J., BLANKENSHIP R. E. and ENGEL G. S., *Proc. Natl. Acad. Sci. USA*, **107** (2010) 12766.
- [3] FLEMING G. R., SCHOLES G. D. and CHENG Y.-C., *Procedia Chemistry*, (2011) 22nd Solvay Conference in Chemistry.
- [4] OLBRICH C., STRÜMPFER J., SCHULTEN K. and KLEINEKATHÖFER U., *J. Phys. Chem. B*, **115** (2011) 758.
- [5] FENNA R. E. and MATTHEWS B. W., *Nature*, **258** (1975) 573.
- [6] VAN AMERONGEN H., VALKUNAS L. and VAN GRONDELLE R., *Photosynthetic Excitons* (World Scientific, Singapore) 2000.
- [7] CHENG Y.-C. and FLEMING G. R., *Annu. Rev. Phys. Chem.*, **60** (2009) 241.
- [8] REBENTROST P., MOHSENI M. and ASPURU-GUZIĆ A., *J. Phys. Chem. B*, **113** (2009) 9942.
- [9] CHIN A. W., DATTA A., CARUSO F., HUELGA S. F. and PLENIĆ M. B., *New J. Phys.*, **12** (2010) 065002.
- [10] WU J., LIU F., SHEN Y., CAO J. and SILBEY R. J., *New J. Phys.*, **12** (2010) 105012.
- [11] ADOLPHS J. and RENGER T., *Biophys. J.*, **91** (2006) 2778.
- [12] ABRAMAVICIUS D. and MUKAMEL S., *J. Chem. Phys.*, **133** (2010) 064510.
- [13] HUGHES K. H., CHRIST C. D. and BURGHARDT I., *J. Chem. Phys.*, **131** (2009) 124108.
- [14] THORWART M., ECKEL J., REINA J., NALBACH P. and WEISS S., *Chem. Phys. Lett.*, **478** (2009) 234 .
- [15] LIANG X.-T., *Phys. Rev. E*, **82** (2010) 051918.
- [16] SAROVAR M., ISHIZAKI A., FLEMING G. R. and WHALEY K. B., *Nat. Phys.*, **6** (2010) 462.
- [17] MÜLKEN O., MÜHLBACHER L., SCHMID T. and BLUMEN A., *Phys. Rev. E*, **81** (2010) 041114.
- [18] CAI J., POPESCU S. and BRIEGEL H.-J., *Phys. Rev. E*, **82** (2010) 021921.
- [19] ALICKI R. and GIRALDI F., *arXiv:1103.0554*, (2011) .
- [20] WÜSTER S., ATEŞ C., EISFELD A. and ROST J.-M., *Phys. Rev. Lett.*, **105** (2010) 053004.
- [21] SCHOLAK T., MINTERT F., WELLENS T. and BUCHLEITNER A., *Semiconductors and Semimetals*, **83** (2010) 1.
- [22] SCHOLAK T., DE MELO F., WELLENS T., MINTERT F. and BUCHLEITNER A., *Phys. Rev. E*, **83** (2011) 021912.
- [23] ARNDT M., BUCHLEITNER A., MANTEGNA R. N. and WALTHER H., *Phys. Rev. Lett.*, **67** (1991) 2435.
- [24] KRAMER B. and MACKINNON A., *Rep. Prog. Phys.*, **56** (1993) 1469.